

# Biosynthesis of Ursolic Acid and Oleanolic Acid in *Saccharomyces cerevisiae*

Chunzhe Lu<sup>†</sup>, Chuanbo Zhang<sup>†</sup>, Fanglong Zhao and Dashuai Li

Dept. of Biological Engineering, School of Chemical Engineering and Technology, Tianjin University, Tianjin, 300072, China

Wenyu Lu\* 

Dept. of Biological Engineering, School of Chemical Engineering and Technology, Tianjin University, Tianjin, 300072, China and Key Laboratory of system bioengineering (Tianjin University), Ministry of Education, Tianjin, 300072, China and Collaborative Innovation Center of Chemical Science and Engineering (Tianjin), Tianjin, 300072, China

DOI 10.1002/aic.16370

Published online August 27, 2018 in Wiley Online Library (wileyonlinelibrary.com)

*Ursolic acid and oleanolic acid are pentacyclic triterpenoid compounds with a variety of biological activities. A mixture of ursolic acid and oleanolic acid has higher antitumor activity than the individual acids. We have developed a simultaneous biosynthesis pathway for different proportions of ursolic acid and oleanolic acid in Saccharomyces cerevisiae. The ScLCZ08 strain produced 175.15 mg/L of the ursolic acid precursor  $\alpha$ -amyrin, the highest amount reported. Ursolic and oleanolic acid titers and proportions were optimized using Medicago truncatula amyirin C-28 oxidase and Arabidopsis thaliana cytochrome P450 reductase. Using glucose and ethanol fed-batch fermentation strategies, the final ursolic acid and oleanolic acid titers were 123.27 and 155.58 mg/L, respectively, demonstrating 4.77-fold and 4.95-fold higher production than the parent strain. The ScLCZ11 strain displayed the highest ursolic acid production obtained via microbial fermentation in fed-batch culture to date. © 2018 American Institute of Chemical Engineers AIChE J, 64: 3794–3802, 2018*

**Keywords:** ursolic acid, oleanolic acid,  $\alpha$ -amyrin,  $\beta$ -amyrin, *Saccharomyces cerevisiae*

## Introduction

Ursolic acid (UA) and its isomer, oleanolic acid (OA), are widely distributed in plants and fruits.<sup>1–4</sup> Ursolic acid exhibits a variety of biological activities, including anti-inflammatory,<sup>5</sup> anti-oxidation,<sup>6</sup> antidiabetic,<sup>7</sup> antibacterial,<sup>8</sup> antimetastatic,<sup>9</sup> antiangiogenic,<sup>10</sup> and antitumorigenic activities.<sup>11</sup> Oleanolic acid possesses many of these activities, and its most important pharmacological activity is its remarkable hepatoprotective effect.<sup>12,13</sup> Besides, ursolic acid and oleanolic acid show the synergistic activity; a mixture of the two acids (UA/OA = 1:1) possesses higher antitumor and antimicrobial activities than those of the individual acids.<sup>14</sup>

The various biological activities of ursolic acid and oleanolic acid and their pharmacological mechanisms have attracted the interest of many researchers. However, only a few studies have been performed regarding their biosynthesis, and their main source for commercial and industrial application is still plant extraction.<sup>4,15</sup> Two triterpene biosynthesis pathways have been reported in plants: the methylerythritol-phosphate pathway (MEP) and the mevalonate pathway (MVA). In *Saccharomyces cerevisiae*, triterpene acids are synthesized via glycolysis and the MVA pathway. Mevalonate is converted

into isopentenyl diphosphate (IPP) and its isomer dimethylallyl diphosphate (DMAPP) via multiple reactions. The reduction of hydroxymethylglutaryl (HMG)-CoA by HMG-CoA reductase to generate mevalonate is a key limited step. Biosynthesis of the triterpene skeleton begins with the condensation of DMAPP and 2 IPP molecules, producing farnesyl diphosphate (FPP). Two molecules of FPP are condensed to produce squalene, which is subsequently converted into 2,3-oxidosqualene, a common precursor of the triterpene skeletons,  $\alpha$ -amyrin and  $\beta$ -amyrin, by squalene monooxygenase. Heterologous biosynthesis of ursolic acid and oleanolic acid was previously accomplished in *S. cerevisiae* by introducing multifunctional amyirin synthase, amyirin C-28 oxidase, and cytochrome P450 reductase (CPR), but the yields were low, especially for ursolic acid. The BY-OA strain constructed by Dai et al., produced 71.0 mg/L oleanolic acid.<sup>16</sup> However, yeast cells expressing CrAS/CrAO only produced 0.1 mg/L ursolic acid and 0.045 mg/L oleanolic acid.<sup>17</sup> The cyclization of 2,3-oxidosqualene is the key step in pentacyclic triterpene biosynthesis. Monofunctional  $\beta$ -amyirin synthases have been identified in many different plants.<sup>18–22</sup> For example, the  $\beta$ -amyirin synthase from *Glycyrrhiza glabra* has been expressed in *S. cerevisiae* to produce  $\beta$ -amyirin.<sup>23</sup> However, no monofunctional  $\alpha$ -amyirin synthase has been found, and some researchers believe that such an enzyme does not exist in nature.<sup>24–26</sup> The compounds,  $\alpha$ -amyirin and  $\beta$ -amyirin, not only display many bioactivities,<sup>27–29</sup> but can also be further transformed into triterpenoids and saponins:  $\alpha$ -amyirin can be

Additional Supporting Information may be found in the online version of this article.

<sup>†</sup>These authors contributed equally to this work.

Correspondence concerning this article should be addressed to W. Lu at wenyulu@tju.edu.cn.

converted to ursolic acid and centellosides, and  $\beta$ -amyrin can be oxidized to biologically active compounds such as oleanolic acid and glycyrrhetic acid.

Cytochrome P450 enzymes, dehydrogenases, and other functional enzymes can further modify the triterpenoid skeleton. A number of cytochrome P450 enzymes related to triterpene biosynthesis have been confirmed. CYP88D6 from *G. glabra* catalyzes the C-11 oxidation of  $\beta$ -amyrin during glycyrrhetic acid biosynthesis.<sup>30</sup> CYP716AL1 from *Catharanthus roseus* is responsible for catalyzing a three-step successive oxidation reaction at the C-28 positions of  $\alpha$ -amyrin and  $\beta$ -amyrin, producing ursolic acid and oleanolic acid, respectively.<sup>17</sup> CYP716A12 from *Medicago truncatula*<sup>31</sup> and CYP716A15 and CYP716A17 from *Vitis vinifera* possess the same catalytic activity as CYP716AL1.<sup>4</sup> Three-step successive oxidation appears to be common in terpene synthesis. Several enzymes, such as *Pinus taeda* CYP720B1 in resin acid biosynthesis<sup>32</sup> and *Artemisia annua* CYP71AV1 in artemisinin biosynthesis<sup>33</sup> catalyze successive oxidation reactions.

In this study, we aimed to efficiently synthesize ursolic acid and oleanolic acid in *S. cerevisiae* (Figure 1). To increase the yields, precursor supplies were enhanced by overexpressing key enzymes in the MVA pathway, and electron transfer efficiency was optimized by combining plant cytochrome P450 enzymes and different P450 reductases. The production of ursolic acid in engineered yeast is a potential alternative to plant extraction. The results of this study provide a framework for the production of various pentacyclic triterpenes, which could be used in anticancer research.

## Materials and Methods

### Strains, genes, vectors, and media

*S. cerevisiae* W303-1a was used as the host strain for all engineered yeast strains. Engineered yeast strains were cultured in SD medium<sup>34</sup> lacking adenine, histidine, leucine, and uracil where appropriate, and then grown in yeast extract peptone dextrose (YPD) medium. *Escherichia coli* Trans1-T1 cells (Transgen Biotech, Beijing, China) were used for plasmid DNA extraction and gene transformation. All constructed plasmids are listed in Supporting Information Table S1. The pRS304, pRS405, and pXP320 plasmids were acquired from the American Type Culture Collection. Genes (*CrMAS* (GenBank: JN991165), *CrOAS* (GenBank: JN565975), *MtOAS* (GenBank: ABC59076.1), *AtCPR1* (GenBank: BT008426.1), and *LjCPR1* (GenBank: AB433810.1)) were synthesized by GENECREATE (Wuhan, China) with codon optimization. The synthesized genes were cloned into the pUC57 vector to generate the p-CrMAS, p-CrOAS, p-MtOAS, p-AtCPR1, and p-LjCPR1 plasmids, respectively.

### Plasmid and strain construction

The *tHMG1*, *ERG20*, and *ScERG1* genes were cloned from *S. cerevisiae* W303-1a. *CaERG1* was cloned from *Candida albicans*. Primers used for plasmid and strain construction are summarized in Supporting Information Tables S2-S5. Yeast promoters ( $P_{PGK1}$ ,  $P_{TEF1}$ ,  $P_{GAL1}$ ,  $P_{TDH3}$ ) and terminators ( $T_{CYC1}$ ,  $T_{ADH1}$ ,  $T_{ADH3}$ ) were amplified from the genomic DNA of *S. cerevisiae* W303-1a. The *CrMAS*, *CrOAS*, *MtOAS*, *AtCPR1*, and *LjCPR1* genes were amplified from the p-CrMAS, p-CrOAS, p-MtOAS, p-AtCPR1, and p-LjCPR1 plasmids, respectively. *CrMAS* was subcloned into plasmid pXP320 using SpeI and XhoI sites to produce pXP320-*CrMAS*. The gene expression cassette  $P_{TDH3}$ -

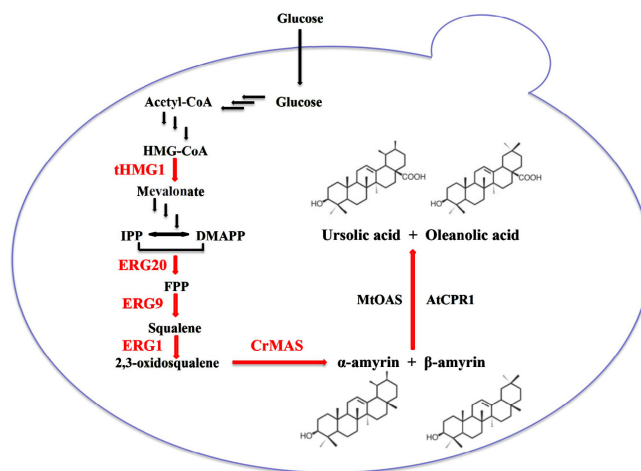


**Figure 1. Biosynthetic pathway of ursolic acid and oleanolic acid in engineered *Saccharomyces cerevisiae*.**

Truncated 3-hydroxy-3-methylglutaryl coenzyme A reductase (*tHMG1*), farnesyl diphosphate synthetase (*ERG20*), squalene monooxygenase (*ERG1*), multifunctional amyryn synthase from *Catharanthus roseus* (*CrMAS*), amyryn C-28 oxidase from *Medicago truncatula* (*MtOAS*), and cytochrome P450 reductase from *Arabidopsis thaliana* (*AtCPR1*) were overexpressed in *S. cerevisiae*. IPP, isopentenyl pyrophosphate; DMAPP, dimethylallyl pyrophosphate; FPP, farnesyl diphosphate. [Color figure can be viewed at [wileyonlinelibrary.com](http://wileyonlinelibrary.com)]

*tHMG1-T<sub>CYC1</sub>* was digested with ApaI and PstI, and ligated into the corresponding sites in pRS304 to produce pRS304-*tHMG1*. The gene expression cassette  $P_{PGK1}$ -*ERG20-T<sub>CYC1</sub>* was digested with PstI and BamHI, and ligated into pRS405 to produce pRS405-*ERG20*.

The standard lithium acetate method was used for *S. cerevisiae* transformations.<sup>35</sup> Each gene expression cassette was developed by overlap extension PCR.<sup>36</sup> *S. cerevisiae* strain WTE was constructed by sequentially transforming the recombinant plasmids pRS304-*tHMG1* and pRS405-*ERG20* into *S. cerevisiae* W303-1a. The ScLCZ01 and ScLCZ02 strains were constructed by transforming an empty vector (pXP320) and the pXP320-*CrMAS* construct into *S. cerevisiae* WTE, respectively. All expression cassettes ( $P_{PGK1}$ -*CrMAS-T<sub>ADH1</sub>*,  $P_{PGK1}$ -*CrMAS-T<sub>CYC1</sub>*,  $P_{TEF1}$ -*ScERG1-T<sub>ADH1</sub>*,  $P_{TEF1}$ -*CaERG1-T<sub>ADH1</sub>*,  $P_{GAL1}$ -*CrMAS-T<sub>ADH1</sub>*,  $P_{GAL1}$ -*CrMAS-T<sub>CYC1</sub>*,  $P_{PGK1}$ -*AtCPR1-T<sub>ADH3</sub>*,  $P_{PGK1}$ -*AtCPR1-T<sub>CYC1</sub>*,  $P_{TDH3}$ -*MtOAS-T<sub>ADH3</sub>*,  $P_{PGK1}$ -*LjCPR1-T<sub>ADH3</sub>*,  $P_{PGK1}$ -*LjCPR1-T<sub>CYC1</sub>*, and  $P_{TDH3}$ -*CrOAS-T<sub>ADH3</sub>*) were constructed by fusion PCR. The construction strategy for the genome-integrated strains ScLCZ03-14 is illustrated in Figure 2. All developed strains are listed in Table 1.

### Quantification of genes copy numbers in *S. cerevisiae* by qPCR

According to the absolute quantification method,<sup>37</sup> copy numbers of genes were quantified by qPCR. Open reading frames of *ScERG1*, *CaERG1*, *CrMAS*, *MtOAS*, *CrOAS*, *LjCPR1*, *AtCPR1*, and *ARG4* were amplified and quantified to draw standard curves, respectively. The housekeeping gene *ARG4* was selected as a reference gene. The TIANamp Yeast DNA kit (Tiangen, Beijing, China) was used to extract the genomic DNA of the different colonies. Based on Zhang's description,<sup>38</sup> TaqMan probe-based determinations were

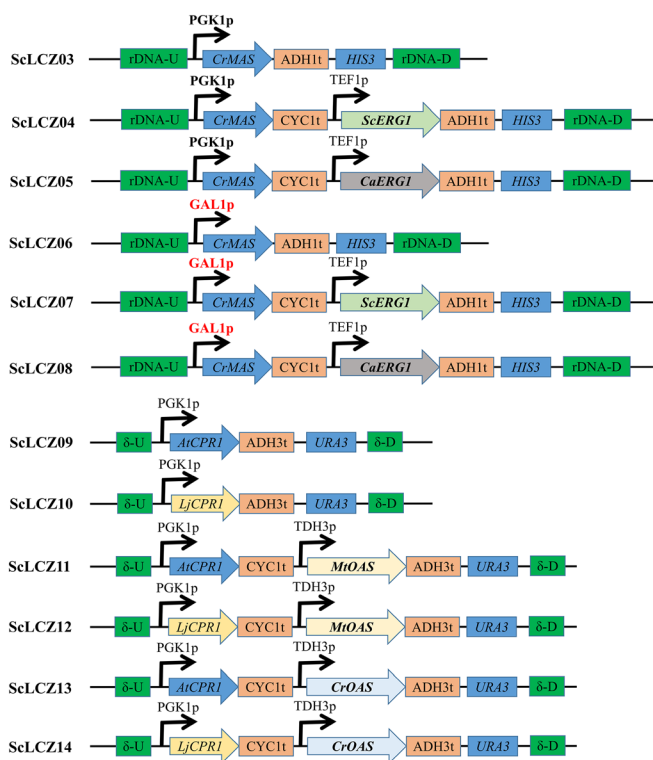


**Figure 2. Construction strategy for engineered strains ScLCZ03-14.**

The black arrows, arrow boxes, orange boxes, and blue boxes represent the promoters, target genes, terminators, and selective markers, respectively. [Color figure can be viewed at [wileyonlinelibrary.com](http://wileyonlinelibrary.com)]

conducted. Primers used for the qPCR are summarized in Supporting Information Table S6.

### Extraction, identification, and quantitation of metabolites

Yeast cultures (5 mL) were centrifuged for 10 min at  $5000 \times g$ . The cells were washed twice with sterile water and then resuspended in 1 mL hexane and vortexed with quartz sand. The hexane phase was derivatized as previously described before gas chromatography-mass spectrometry (GC-MS) analysis.<sup>17</sup> The culture supernatant was extracted with 5 mL ethyl acetate at 30°C and 200 rpm for 12 h. The ethyl acetate phase was evaporated for 5 min, and then resuspended in 1 mL ethyl acetate and used in high-performance liquid chromatography (HPLC) analysis. Squalene,  $\alpha$ -amyrin,  $\beta$ -amyrin, ursolic acid, and oleanolic acid standards were purchased from Sigma-Aldrich (Shanghai, China).

GC-MS analysis was performed on an Agilent 7890A GC machine and an Agilent 5975C mass selective detector with an HP-5ms column (0.25 mm  $\times$  30 m  $\times$  0.25  $\mu$ m). Each sample (1  $\mu$ L) was analyzed with a 20:1 split ratio. The carrier gas was helium, at a flow rate of 1 mL/min. The injection temperature was 250°C. The GC oven temperature was set to 80°C for 2 min after injection, followed by a 20°C/min ramp up to 260°C, then a 5°C/min ramp up to 290°C, and a hold at 290°C for 10 min. Full mass spectra were generated for metabolite identification by scanning the  $m/z$  range of 50-500. Metabolite retention times and mass spectra were compared with those of authentic standards for compound identification.

HPLC analysis was performed on an Elite P230II high-pressure pump system equipped with UV detection at 210 nm.

A Grace Apollo C18 column (250 mm  $\times$  4.6 mm  $\times$  5  $\mu$ m) was used with methyl alcohol/acetonitrile (V/V = 60:40) as the mobile phase at a flow rate of 0.8 mL/min. Liquid chromatography-mass spectrometry (LC-MS) analysis was performed on a surveyor LC system (Thermo Finnigan, San Jose, CA) and an Agilent Zorbax SB Aq column (100 mm  $\times$  2.1 mm  $\times$  3  $\mu$ m) with an electrospray ionization interface. Samples were analyzed in negative ionization mode. Metabolite retention times and mass spectra were compared with those of authentic standards for compound identification.

### Yeast cultivation and fed-batch fermentation

YPD medium was used to cultivate yeast strains WTE and ScLCZ01-14. All strains were inoculated into 250-mL flasks containing 30 mL medium and cultured at 30°C and 220 rpm for 5 days. Shake flask fermentations of all strains were performed in triplicate. The error bars in the figures represent standard deviations of duplicate experiments.

Strains ScLCZ08 and ScLCZ11 were selected for fed batch fermentation in a 5 L fermenter (BaoXing, China). A seed culture was obtained by inoculating a single colony into a 500-mL flask containing 100 mL YPD medium, and culturing at 30°C for 24 h. A 10% (v/v) seed culture was inoculated into a 5-L fermenter containing 2 L YPD medium. Fermentation was performed at 30°C with an initial pH of 5.0. The airflow rate was 4 L/min. The dissolved oxygen was controlled at 35% and pH was maintained at 5.0 with ammonium hydroxide (4 M).

**Table 1. Strains Constructed in This Study**

Strain name	Description
W303-1a	<i>MATa {leu2-3,112 trp1-1 can1-100 ura3-1 ade2-1 his3-11,15}</i>
WTE	Plasmids pRS403- <i>tHMG1</i> and pRS405- <i>ERG20</i> were transformed into W303-1a
ScLCZ01	WTE was transformed with the empty plasmid pXP320
ScLCZ02	WTE was transformed with the plasmid pXP320- <i>CrMAS</i>
ScLCZ03	<i>CrMAS</i> controlled by the <i>PGK1</i> promoter and marker <i>HIS3</i> gene expression cassettes were integrated into the <i>rDNA</i> site of WTE
ScLCZ04	<i>CrMAS</i> controlled by the <i>PGK1</i> promoter, <i>ScERG1</i> and marker <i>HIS3</i> gene expression cassettes were integrated into the <i>rDNA</i> site of WTE
ScLCZ05	<i>CrMAS</i> controlled by the <i>PGK1</i> promoter, <i>CaERG1</i> and marker <i>HIS3</i> gene expression cassettes were integrated into the <i>rDNA</i> site of WTE
ScLCZ06	<i>CrMAS</i> controlled by the <i>GAL1</i> promoter and marker <i>HIS3</i> gene expression cassettes were integrated into the <i>rDNA</i> site of WTE
ScLCZ07	<i>CrMAS</i> controlled by the <i>GAL1</i> promoter, <i>ScERG1</i> and marker <i>HIS3</i> gene expression cassettes were integrated into the <i>rDNA</i> site of WTE
ScLCZ08	<i>CrMAS</i> controlled by the <i>GAL1</i> promoter, <i>CaERG1</i> and marker <i>HIS3</i> gene expression cassettes were integrated into the <i>rDNA</i> site of WTE
ScLCZ09	<i>AiCPR1</i> and marker <i>URA3</i> gene expression cassettes were integrated into the $\delta$ site of ScLCZ08
ScLCZ10	<i>LjCPR1</i> and marker <i>URA3</i> gene expression cassettes were integrated into the $\delta$ site of ScLCZ08
ScLCZ11	<i>AiCPR1</i> , <i>MiOAS</i> , and marker <i>URA3</i> gene expression cassettes were integrated into the $\delta$ site of ScLCZ08
ScLCZ12	<i>AiCPR1</i> , <i>CrOAS</i> , and marker <i>URA3</i> gene expression cassettes were integrated into the $\delta$ site of ScLCZ08
ScLCZ13	<i>LjCPR1</i> , <i>MiOAS</i> , and marker <i>URA3</i> gene expression cassettes were integrated into the $\delta$ site of ScLCZ08
ScLCZ14	<i>LjCPR1</i> , <i>CrOAS</i> , and marker <i>URA3</i> gene expression cassettes were integrated into the $\delta$ site of ScLCZ08



The fed batch fermentation process consisted of two stages, the cell growth stage and the target product synthesis stage. In the cell growth stage, glucose was used as a carbon source for fermentation. Concentrated glucose solution (600 g/L, 1000 mL) was intermittently poured into the fermenters to maintain the glucose concentration under 2 g/L. Vitamins (12 mL/L, 24 mL) and trace metal (10 mL/L, 20 mL) solutions, prepared as previously described,<sup>39</sup> were mixed with the glucose solution. At 60 h, D-(+)-galactose (600 g/L, 200 mL) at a final concentration of 40 g/L was added to induce the biosynthesis of ursolic acid and oleanolic acid. In the meantime, adenine and uracil (150 g/L, 100 mL) at a final concentration of 5 g/L were added to the fermenter. For the biosynthesis stage, ethanol was used as a carbon source. The ethanol concentration was maintained at less than 5 g/L by controlling the feeding rate of the anhydrous ethanol. Fed-batch fermentation was performed in triplicate.

## Results and Discussion

### *Increasing the squalene supply for amyirin production in *S. cerevisiae**

Squalene is an important precursor of triterpenes, and previous studies have shown that triterpene overproduction is limited by squalene supply.<sup>40,41</sup> As an important rate-limiting enzyme, the HMG-CoA reductase gene is usually truncated to increase its enzyme activity, thus allowing yeast to accumulate large amounts of squalene. Overexpression of key rate limiting enzymes in the MVA metabolic pathway is a common method to increase terpenoid production. This method has been successfully applied for the production of various terpenoids (sesquiterpenoids, diterpenoids, and triterpenoids).<sup>16</sup> In a previous study, increasing squalene supplies increased the titer of  $\beta$ -amyirin by almost 31%.<sup>42</sup> In our study, *tHMG1* and farnesyl diphosphate synthase (*ERG20*) were overexpressed in the *S. cerevisiae* WTE strain. Compared with the parent strain, squalene production increased by 4.82-fold, reaching 165.28 mg/L (Figure 3). Therefore, the *S. cerevisiae* WTE strain was used for the production of  $\alpha$ -amyirin and  $\beta$ -amyirin.

### *$\alpha$ - and $\beta$ -amyirin biosynthesis in *S. cerevisiae**

$\alpha$ -amyirin and  $\beta$ -amyirin are ursane-type and oleanane-type pentacyclic triterpenoid precursors. A multifunctional amyirin synthase from apple (*Malus domestica*) has been expressed in *Pichia methanolica* to produce  $\alpha$ -amyirin (>80%) and  $\beta$ -amyirin.<sup>26</sup> Huang et al. isolated a new hybrid amyirin synthase from *C. roseus*, which they introduced into the *S. cerevisiae* WAT11 strain.<sup>17</sup>  $\alpha$ -amyirin and  $\beta$ -amyirin were detected in hexane extracts, but with low titers.

A number of oxidosqualene cyclases that can simultaneously synthesize both  $\alpha$ -amyirin and  $\beta$ -amyirin have been reported.<sup>43,44</sup> In this study, the multifunctional amyirin synthase *CrMAS* from *C. roseus* was expressed in plasmid pXP320, to generate the ScLCZ02 strain, for  $\alpha$ -amyirin and  $\beta$ -amyirin production in *S. cerevisiae*. Moreover, *CrMAS*, controlled by the *PGK1* or *GAL1* promoters, was integrated into the chromosomes of the WTE strain at rDNA sites to generate the ScLCZ03 and ScLCZ06 strains, respectively. Hexane extracts from the ScLCZ01 and ScLCZ02 strains were analyzed by GC-MS. The presence of  $\alpha$ -amyirin and  $\beta$ -amyirin was confirmed using corresponding chemical standards (Figure 4a, b). The ScLCZ02, ScLCZ03, and ScLCZ06 strains produced 4.89, 1.51, and 5.64 mg/L  $\alpha$ -amyirin and 1.36, 0.46, and 1.64 mg/L  $\beta$ -amyirin, respectively (Figure 4c). With the

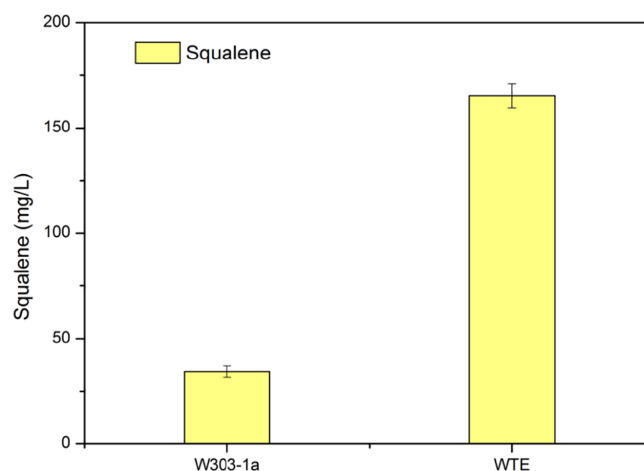


**Figure 3. Squalene production by the W303-1a and WTE strains.**

[Color figure can be viewed at wileyonlinelibrary.com]

highest  $\alpha$ -amyirin and  $\beta$ -amyirin production, ScLCZ06 was used in further optimization experiments. Although the copy number of *CrMAS* in ScLCZ06 was around twice that in ScLCZ03 (Figure 6), the amyirin titer still proved that the *GAL1* promoter is more beneficial to amyirin production than the *PGK1* promoter. Therefore, the *GAL1* promoter was chosen to control the subsequent fermentation process.

### *The effect of heterologous squalene monooxygenase expression on $\alpha$ -amyirin and $\beta$ -amyirin synthesis*

Only 6 mg/L  $\beta$ -amyirin was produced by an engineered *S. cerevisiae* strain constructed by Kirby et al.<sup>45</sup> By introducing the heterologous squalene monooxygenase from *C. albicans* and overexpressing IPP isomerase, FPP synthase, and squalene synthase, the SGib strain constructed by Zhang et al. produced 36.5 mg/L  $\beta$ -amyirin,<sup>42</sup> suggesting that the introduction of a heterologous squalene monooxygenase can effectively increase the titer of mixed amyirin. Squalene epoxidase (*ERG1*), a rate-limiting enzyme in the ergosterol biosynthetic pathway, possesses a low specific activity in *S. cerevisiae*.<sup>46</sup> Squalene is transformed into 2,3-oxidosqualene through *ERG1* catalysis, and then *CrMAS* catalyzes the conversion of 2,3-oxidosqualene to  $\alpha$ -amyirin and  $\beta$ -amyirin. A previous research has shown that *C. albicans* *ERG1* exhibits higher activity than the endogenous *S. cerevisiae* *ERG1*.<sup>47</sup> We overexpressed *ScERG1* and *CaERG1* in the ScLCZ03 and ScLCZ06 strains to generate the ScLCZ04, ScLCZ05, ScLCZ07, and ScLCZ08 strains.

As shown in Figure 5, the ScLCZ08 strain produced 25.99 mg/L  $\alpha$ -amyirin, an increase of 3.6-fold compared with ScLCZ06, while the ScLCZ07 strain produced 19.43 mg/L  $\alpha$ -amyirin, a 2.4-fold increase compared with ScLCZ06. However, the transcription level of *ScERG1* in ScLCZ07 was 1.2-fold higher than that of *CaERG1* in ScLCZ08 (Figure 6). Therefore, *CaERG1* from *C. albicans* was a better enzyme for mixed amyirin production than *ERG1* from *S. cerevisiae*.

### *Increasing amyirin production in shake flask and fed batch fermentation*

The enzymatic activity of the cytochrome P450 enzymes used in ursolic acid and oleanolic acid synthesis is not high.<sup>4</sup> Therefore, we increased precursor production by optimizing the fermentation conditions. Figure 7a,b shows the effects of

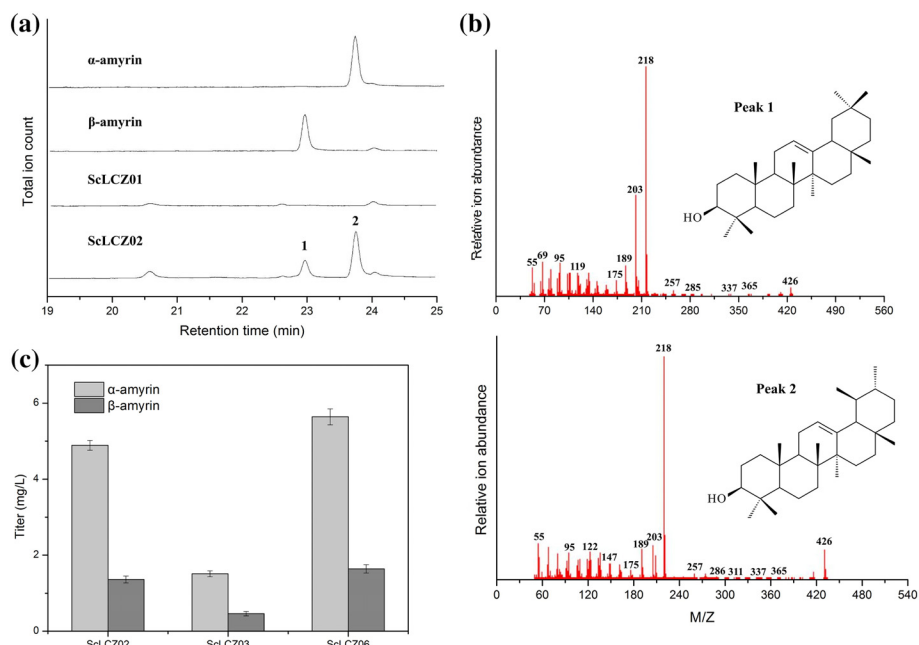
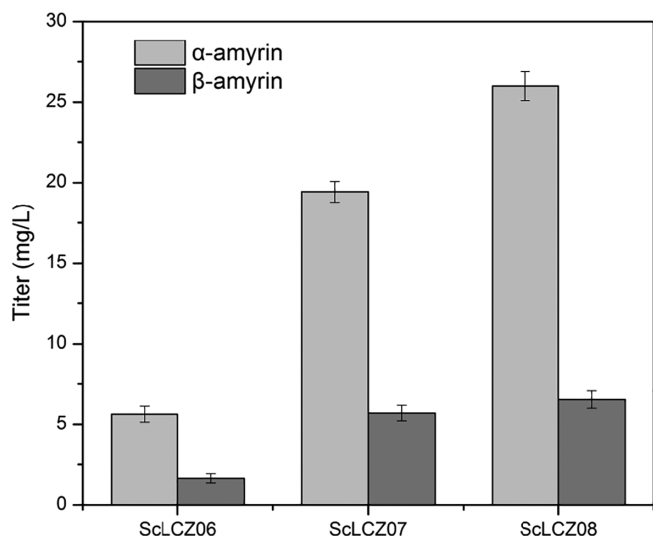


**Figure 4. Gas chromatography-mass spectrometry analysis of  $\alpha$ -amyrin and  $\beta$ -amyrin produced by engineered yeast.**

(a) Gas chromatograms of  $\alpha$ -amyrin and  $\beta$ -amyrin standards and *n*-hexane extracts from ScLCZ01 and ScLCZ02 cells. (b) Mass spectra of peaks 1 and 2. (c) Amyrin production in the ScLCZ02, ScLCZ03, and ScLCZ06 strains. [Color figure can be viewed at [wileyonlinelibrary.com](#)]

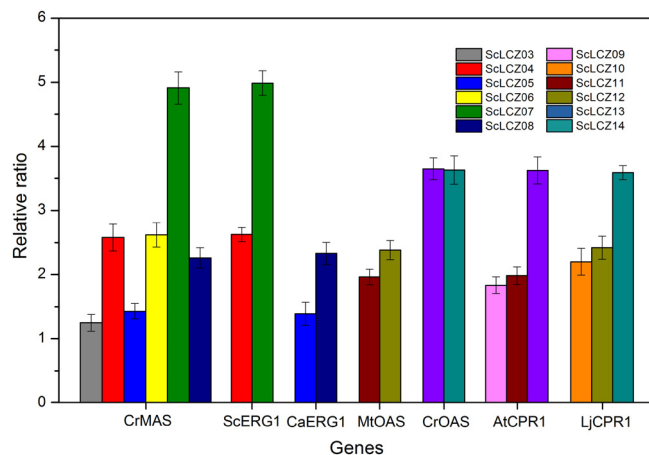
glucose and galactose concentrations on the titer of  $\alpha$ -amyrin and  $\beta$ -amyrin. Increasing the initial glucose concentration increased the titer of  $\alpha$ -amyrin from 26.05 mg/L at 20 g/L to 40.15 mg/L at 30 g/L, while higher initial glucose concentrations decreased the titer (25.28 mg/L at 50 g/L). The  $\beta$ -amyrin titer displayed the same trend. Increased galactose concentrations gradually increased the  $\alpha$ -amyrin titer from 9.35 mg/L at 5 g/L to 30.52 mg/L at 50 g/L and  $\beta$ -amyrin titer from 3.18 mg/L at 5 g/L to 7.12 mg/L at 50 g/L.

Adenine and uracil are both important components for yeast cell growth. However, due to the absence of corresponding genes in the engineered yeast, these two compounds cannot be synthesized spontaneously. Therefore, it is necessary to introduce them to the reaction during the fermentation process.



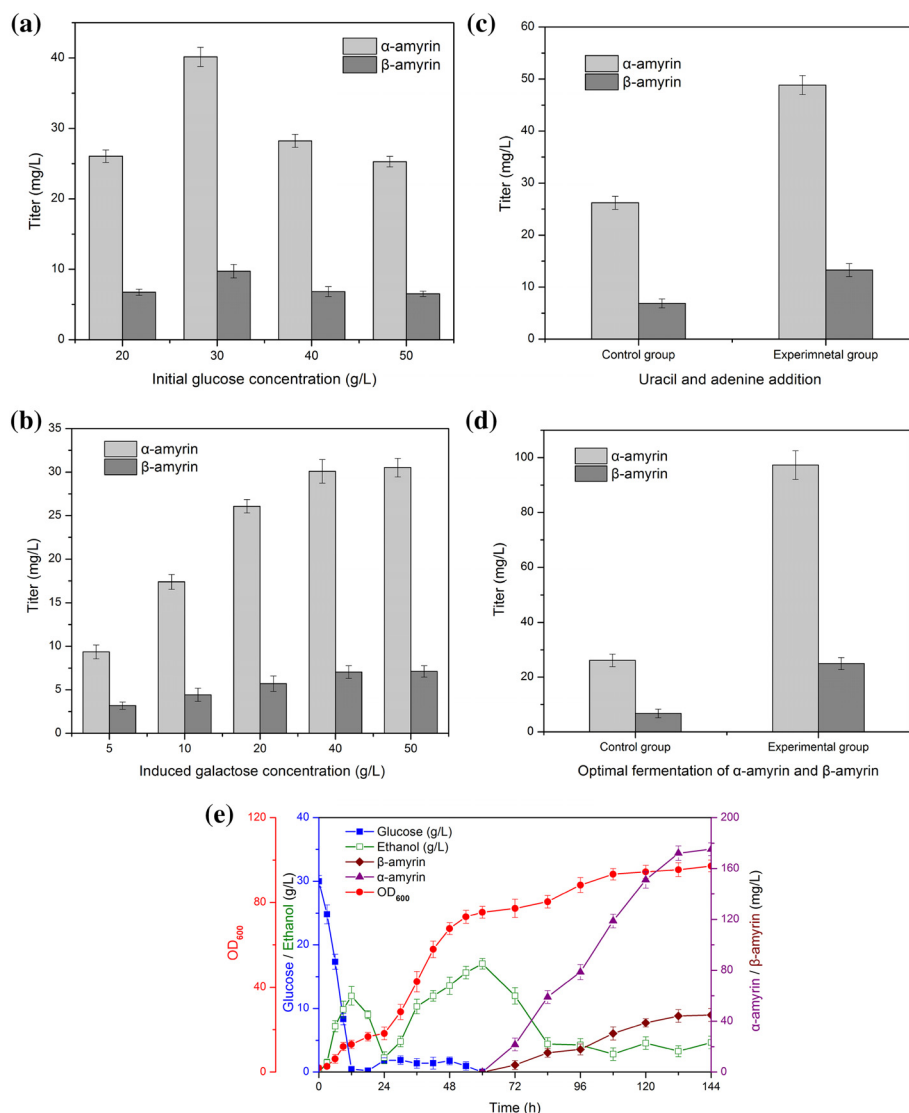
**Figure 5. Production of  $\alpha$ -amyrin and  $\beta$ -amyrin by the engineered ScLCZ06–08 strains.**

Figure 7c shows the effects of adenine and uracil addition on the titers of  $\alpha$ -amyrin and  $\beta$ -amyrin. The  $\alpha$ -amyrin titer reached 48.83 mg/L, an 86.3% increase compared to the control, and the  $\beta$ -amyrin titer reached 13.28 mg/L, a 93.3% increase compared to the control. In conclusion, with increased initial glucose and galactose inducer concentrations and the addition of adenine and uracil, the titers of  $\alpha$ -amyrin and  $\beta$ -amyrin increased. When strain ScLCZ08 was cultivated in YPD medium with 30 g/L glucose, 40 g/L galactose, and 5 g/L mixture of uracil and adenine, it achieved the maximum titer for  $\alpha$ -amyrin and  $\beta$ -amyrin. As shown in Figure 7d, the ScLCZ08 strain produced 97.31 mg/L  $\alpha$ -amyrin and 24.95 mg/L  $\beta$ -amyrin under optimal fermentation conditions. When strain ScLCZ08 was cultured in a 5 L fermenter by using the glucose and ethanol fed-batch fermentation mode, it



**Figure 6. Transcriptional quantification of genes determined *via* qPCR.**

[Color figure can be viewed at [wileyonlinelibrary.com](#)]



**Figure 7.** Effects of initial glucose concentration (a), galactose inducer concentration (b), and uracil and adenine addition (c) on  $\alpha$ - and  $\beta$ -amyirin production in the ScLCZ08 strain. In (c), uracil and adenine were not added to the control group. (d)  $\alpha$ - and  $\beta$ -amyirin production by the ScLCZ08 strain under optimized fermentation conditions. The control group was fermented with 20 g/L glucose, 20 g/L galactose, and no added uracil and adenine. (e)  $\alpha$ -amyirin and  $\beta$ -amyirin production in fed-batch fermentation. [Color figure can be viewed at [wileyonlinelibrary.com](http://wileyonlinelibrary.com)]

produced 175.15 mg/L  $\alpha$ -amyirin and 44.92 mg/L  $\beta$ -amyirin (Figure 7e). To the best of our knowledge, 175.15 mg/L  $\alpha$ -amyirin is the highest titer produced by a microbial cell factory to date.

### Construction of ursolic acid and oleanolic acid biosynthesis pathways in *S. cerevisiae*

To construct ursolic acid and oleanolic acid synthetic pathways in *S. cerevisiae*, two different amyirin C-28 oxidase genes (*MtOAS* and *CrOAS*, from *M. truncatula* and *C. roseus*, respectively; controlled by the TDH3 promoter), and two different CPR genes (*AtCPR1* and *LjCPR1*, from *A. thaliana* and *L. japonicus*, respectively; controlled by the PGK1 promoter) were integrated into the chromosome of the ScLCZ08 strain at the  $\delta$  site to generate the ScLCZ11, ScLCZ12, ScLCZ13, and ScLCZ14 strains. Ethyl acetate extracts from fermentation broths of the ScLCZ09-14 strains were analyzed by LC-MS.

Ursolic acid and oleanolic acid were confirmed using the corresponding chemical standards (Figure 7a,b). Ursolic acid production in the ScLCZ11, ScLCZ12, ScLCZ13, and ScLCZ14 strains was 25.85, 24.58, 23.37, and 22.96 mg/L, respectively, and oleanolic acid production in the four strains was 31.41, 29.49, 24.34, and 23.91 mg/L, respectively (Figure 7c). For ursolic acid produced by strains ScLCZ11 and ScLCZ12, respectively, the *P* value was 0.0412. For oleanolic acid produced by strains ScLCZ11 and ScLCZ12, respectively, the *P* value was 0.0382. These two *P* values ( $<.05$ ) indicate that strain ScLCZ11 significantly accumulated more ursolic acid and oleanolic acid than strain ScLCZ12. Strains ScLCZ11 and ScLCZ13 only differ in their possession of amyirin C-28 oxidase. Besides, the transcription level of *CrOAS* in ScLCZ13 was 1.86-fold higher than that of *MtOAS* in ScLCZ11 (Figure 6), whereas strain ScLCZ11 could produce more ursolic acid and oleanolic acid than strain ScLCZ13. These results indicate that *MtOAS* is more suitable for ursolic acid and

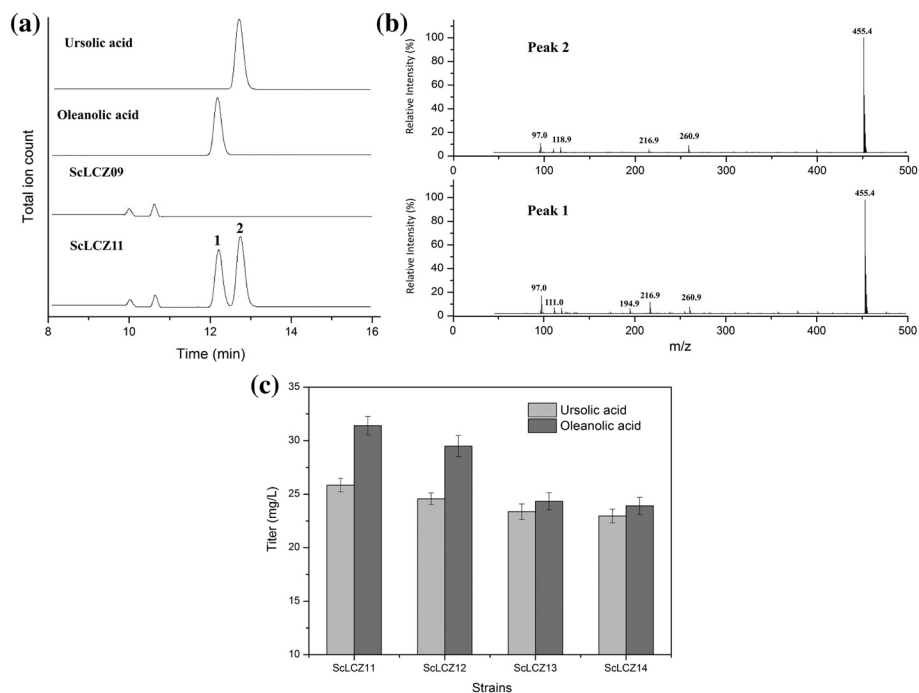


**Figure 8. Liquid chromatography-mass spectrometry analysis of ursolic acid and oleanolic acid production by the engineered *Saccharomyces cerevisiae* strain ScLCZ11.**

(a) Liquid chromatograms of ursolic acid and oleanolic acid standards and ethyl acetate extracts from the fermentation broths of the ScLCZ09 and ScLCZ11 strains. (b) Mass spectra of peaks 1 and 2. (c) Production of ursolic acid and oleanolic acid by the engineered yeast strains ScLCZ11–14.

oleanolic acid synthesis than *CrOAS*. With the highest ursolic acid and oleanolic acid production, the ScLCZ11 strain was used in further optimization experiments.

For the synthesis of valuable triterpenoids, *S. cerevisiae* is a promising host.<sup>16</sup> Compared with plant extraction, heterologous synthesis of triterpenoids in yeast has opened a new path towards obtaining bioactive products. However, to be considered a promising alternative, developed *S. cerevisiae* should produce ursolic acid and oleanolic acid at high yields. Amyrin C-28 oxidase may be the rate-limiting enzyme in oleanolic acid production.<sup>16</sup> CPRs are necessary for cytochrome P450 catalytic activity, through the transfer of electrons from NAD(P)H to the P450 heme center. CPR genes from *A. thaliana* and *L. japonicus* were used in our study.

Many amyrin C-28 oxidases have been identified that can catalyze successive three-step oxidation. Similar oxidation processes exist in the biosynthesis of other terpenoids. For example, amorpha-14:15-diene is oxidized to form artemisinic acid by cytochrome P450 CYP71AV1.<sup>33</sup> By screening efficient dehydrogenases and cytochromes, the production of artemisinic acid was improved to 25 g/L in the reconstructed yeast.<sup>41</sup> To further increase the yield of the desired compound, one practical approach is to identify other novel dehydrogenases and cytochrome enzymes in plants rich in the target product.

#### Simultaneous biosynthesis of ursolic acid and oleanolic acid during fed-batch fermentation

The ScLCZ11 strain was selected for simultaneous biosynthesis of ursolic acid and oleanolic acid in a 5-L fermenter. Cell growth was divided into two stages: in the first stage, glucose was used as carbon source for cell growth without product synthesis; in the second stage, ethanol was used as a carbon source for cell growth and product synthesis following

the addition of the inducer galactose. However, although glucose is more conducive for cell growth, it is rapidly converted to ethanol by yeast when its concentration in the fermenter is excessively high, resulting in a high ethanol concentration, which has an inhibitory effect on cell growth. According to the two-stage culture and carbon source concentration restriction strategy, strain ScLCZ11 produced 123.37 mg/L ursolic acid and 155.58 mg/L oleanolic acid after 168 h of cultivation, with yields of 1.65 and 2.08 mg/g dry cell weight (DCW), respectively (Figure 8). The ScLCZ11 strain had the highest ursolic acid production ever obtained *via* microbial fermentation. However, the yield of oleanolic acid was lower than that in a previous study by Dai et al.<sup>16</sup> This could be attributed to differences in product diversity. Strain BY-OA, constructed by

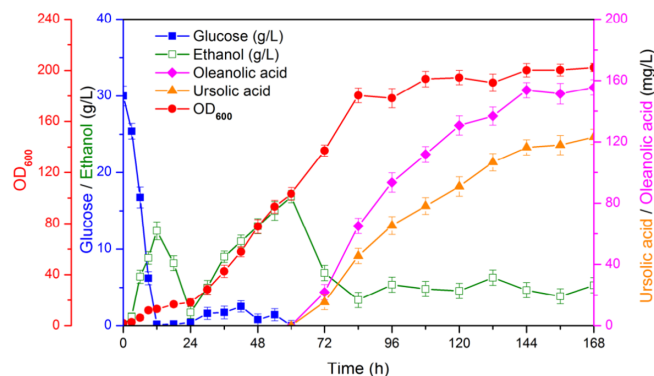


**Figure 9. Profile of cell growth, glucose, ethanol, and the accumulation of ursolic acid and oleanolic acid in the engineered strain ScLCZ11 during fed-batch fermentation.**

[Color figure can be viewed at wileyonlinelibrary.com]

Dai et al., produced only oleanolic acid. Previous studies have shown that ethanol is a beneficial carbon source for terpene production,<sup>37,48,49</sup> possibly because ethanol increases the supply of precursors or enhances the activity of key enzymes in the isoprene metabolic pathway.<sup>48</sup> By identifying and characterizing novel amyirin C-28 oxidases, a large amount of ursolic acid and oleanolic acid with different proportions can be produced using the engineered yeast. The production of ursolic acid and oleanolic acid could also be further increased by using metabolic engineering and fermentation optimization; these strategies will help to meet the requirements for the treatment of various diseases.

## Conclusions

In this work, ursolic and oleanolic acids production was achieved through the metabolic engineering of ursolic acid and oleanolic acid biosynthesis pathways in *S. cerevisiae*. By screening different multifunctional amyirin synthases and amyirin C-28 oxidases, four strains were constructed for simultaneous biosynthesis of ursolic acid and oleanolic acid in different proportions. The ScLCZ11 strain produced 123.37 mg/L ursolic acid and 155.58 mg/L oleanolic acid after 168 h of cultivation with yields of 1.65 and 2.08 mg/g DCW, respectively, under fed-batch fermentation conditions. As far as we know, this is the highest ursolic acid production obtained *via* microbial fermentation to date. Our strategy could be adapted for the overproduction of valuable triterpenes in engineered yeast.

## Acknowledgment

This work was financially supported by the Major Research Plan of Tianjin (No. 16YFXTSF00460) and the National Basic Research Program of China ("973" Program No. 2012CB721105).

## Literature Cited

- Gnoatto SC, Dassonville-klimpt A, Da NS, et al. Evaluation of ursolic acid isolated from *Ilex paraguariensis* and derivatives on aromatase inhibition. *Eur J Med Chem.* 2008;43(9):1865-1877.
- Bamuamba K, Gammon DW, Meyers P, Dijoux-Franca MG, Scott G. Anti-mycobacterial activity of five plant species used as traditional medicines in the western Cape Province (South Africa). *J Ethnopharmacol.* 2008;117(2):385-390.
- Fai YM, Tao CC. A review of presence of oleanolic acid in natural products. *Nat Proda Medica.* 2009;2:77-290.
- Fukushima EO, Seki H, Ohyama K, et al. CYP716A subfamily members are multifunctional oxidases in triterpenoid biosynthesis. *Plant Cell Physiol.* 2011;52(12):2050-2061.
- Baricevic D, Sosa S, Della Loggia R, et al. Topical anti-inflammatory activity of *Salvia officinalis* L. leaves: the relevance of ursolic acid. *J Ethnopharmacol.* 2001;75(2):125-132.
- Saravanan R, Viswanathan P, Pugalendi KV. Protective effect of ursolic acid on ethanol-mediated experimental liver damage in rats. *Life Sci.* 2006;78(7):713-718.
- Ullevig SL, Zhao Q, Zamora D, Asmis R. Ursolic acid protects diabetic mice against monocyte dysfunction and accelerated atherosclerosis. *Atherosclerosis.* 2011;219(2):409-416.
- Kurek A, Markowska K, Grudniak AM, Janiszowska W, Wolska KI. The effect of oleanolic and ursolic acids on the hemolytic properties and biofilm formation of *Listeria monocytogenes*. *Pol J Microbiol.* 2014;63:21-25.
- Xiang L, Chi T, Tang Q, et al. A pentacyclic triterpene natural product, ursolic acid and its prodrug US597 inhibit targets within cell adhesion pathway and prevent cancer metastasis. *Oncotarget.* 2015;6(11):9295-9312.
- Jin H, Pi J, Yang F, et al. Ursolic acid-loaded chitosan nanoparticles induce potent anti-angiogenesis in tumor. *Appl Microb Biotech.* 2016;100(15):6643-6652.
- Rashid S, Dar BA, Majeed R, Hamid A, Bhat BA. Synthesis and biological evaluation of ursolic acid-triazolyl derivatives as potential anti-cancer agents. *Eur J Med Chem.* 2013;66:238-245.
- Yu Z, Sun W, Peng W, Yu R, Li G, Jiang T. Pharmacokinetics in vitro and in vivo of two novel prodrugs of oleanolic acid in rats and its hepatoprotective effects against liver injury induced by CCl<sub>4</sub>. *Mol Pharm.* 2016;13(5):1699-1710.
- Zheng X, Zheng QT, Bo S, et al. Advances in research on hepatoprotective activity and synthesis of oleanolic acid derivatives. *J Appl Biopharm Pharmacokinet.* 2015;3(1):27-33.
- Soica C, Oprean C, Borcan F, et al. The synergistic biologic activity of oleanolic and ursolic acids in complex with hydroxypropyl- $\gamma$ -cyclodextrin. *Molecules.* 2014;19(4):4924-4940.
- Sporn MB, Liby KT, Yore MM, Fu L, Lopchuk JM, Gribble GW. New synthetic triterpenoids: potent agents for prevention and treatment of tissue injury caused by inflammatory and oxidative stress. *J Nat Prod.* 2011;74(3):537-545.
- Dai Z, Wang B, Liu Y, et al. Producing aglycons of ginsenosides in bakers' yeast. *Sci Rep.* 2014;4:3698.
- Huang L, Li J, Ye H, et al. Molecular characterization of the pentacyclic triterpenoid biosynthetic pathway in *Catharanthus roseus*. *Planta.* 2012;236(5):1571-1581.
- Zhao C, Xu T, Liang Y, Ren L, Wang Q, Dou B. Functional analysis of  $\beta$ -amyirin synthase gene in ginsenoside biosynthesis by RNA interference. *Plant Cell Rep.* 2015;34(8):1307-1315.
- Ito R, Masukawa Y, Hoshino T. Purification, kinetics, inhibitors and CD for recombinant  $\beta$ -amyirin synthase from *Euphorbia tirucalli* L and functional analysis of the DCTA motif, which is highly conserved among oxidosqualene cyclases. *FEBS J.* 2013;280(5):1267-1280.
- Jin ML, Lee DY, Um Y, et al. Isolation and characterization of an oxidosqualene cyclase gene encoding a  $\beta$ -amyirin synthase involved in *Polygala tenuifolia* Willd. Saponin biosynthesis. *Plant Cell Rep.* 2014;33(3):511-519.
- Jo HJ, Han JY, Hwang HS, Choi YE.  $\beta$ -Amyirin synthase (EsBAS) and  $\beta$ -amyirin 28-oxidase (CYP716A244) in oleanane-type triterpene saponin biosynthesis in *Eleutherococcus senticosus*. *Phytochemistry.* 2017;135:53-63.
- Ali MM, Krishnamurthy P, El-Hadary MH, et al. Identification and expression profiling of a new  $\beta$ -amyirin synthase gene (GmBAS3) from soybean. *Russ J Plant Phys.* 2016;63(3):383-390.
- Chen H, Liu Y, Zhang X, Zhan X, Liu C. Cloning and characterization of the gene encoding  $\beta$ -amyirin synthase in the glycyrrhizic acid biosynthetic pathway in *Glycyrrhiza uralensis*. *Acta Pharma Sin B.* 2013;3(6):416-424.
- Wang Z, Guhling O, Yao R, et al. Two oxidosqualene cyclases responsible for biosynthesis of tomato fruit cuticular triterpenoids. *Plant Physiol.* 2011;155(1):540-552.
- Basyuni M, Oku H, Inafuku M, et al. Molecular cloning and functional expression of a multifunctional triterpene synthase cDNA from a mangrove species *Kandelia candel* (L.) Druce. *Phytochemistry.* 2006;67(23):2517-2524.
- Cyril B, Yar-Khing Y, Eberhard ED, et al. An unusual plant triterpene synthase with predominant  $\alpha$ -amyirin-producing activity identified by characterizing oxidosqualene cyclases from *Malus domestica*. *FEBS J.* 2011;278:2485-2499.
- El-Hagrassi AM, Ali MM, Osman AF, Shaaban M. Phytochemical investigation and biological studies of *Bombax malabaricum* flowers. *Nat Prod Res.* 2011;25(2):141-151.
- Carretero ME, López-Pérez JL, Abad MJ, et al. Preliminary study of the anti-inflammatory activity of hexane extract and fractions from *Bursera simaruba* (Linneo) Sarg. (Burseraceae) leaves. *J Ethnopharmacol.* 2008;116(1):11-15.
- Lin KW, Huang A, Tu HY, et al. Xanthine oxidase inhibitory triterpenoid and Phloroglucinol from Guttiferaceae plants inhibit growth and induced apoptosis in human NTUB1 cells through a ROS-dependent mechanism. *J Agr Food Chem.* 2011;59(1):407-414.
- Seki H, Ohyama K, Sawai S, et al. Licorice  $\beta$ -amyirin 11-oxidase, a cytochrome P450 with a key role in the biosynthesis of the triterpene sweetener glycyrrhizin. *Proc Natl Acad Sci U S A.* 2008;105(37):14204-14209.
- Carrelli M, Biazzi E, Panara F, et al. *Medicago truncatula* CYP716A12 is a multifunctional oxidase involved in the biosynthesis of hemolytic saponins. *Plant Cell.* 2011;23(8):3070-3081.



32. Ro DK, Arimura GI, Lau SYW, Piers E, Bohlmann J. Loblolly pine abietadienol/abietadienal oxidase PtAO (CYP720B1) is a multifunctional, multisubstrate cytochrome P450 monooxygenase. *Proc Natl Acad Sci U S A*. 2005;102(22):8060-8065.
33. Ro DK, Paradise EM, Ouellet M, et al. Production of the antimalarial drug precursor artemisinic acid in engineered yeast. *Nature*. 2006; 440(7086):940-943.
34. Dai Z, Liu Y, Huang L, Zhang X. Production of miltiradiene by metabolically engineered *Saccharomyces cerevisiae*. *Biotechnol Bioeng*. 2012;109(11):2845-2853.
35. Gietz RD, Woods RA. Transformation of yeast by lithium acetate/single-stranded carrier DNA/polyethylene glycol method. *Method Enzymol*. 2002;350:87-96.
36. Shao Z, Zhao H, Zhao H. DNA assembler, an in vivo genetic method for rapid construction of biochemical pathways. *Nucleic Acids Res*. 2008;37(2):e16.
37. Abad S, Kitz K, Hörmann A, et al. Real-time PCR-based determination of gene copy numbers in *Pichia pastoris*[J]. *Biotech J*. 2010;5(4): 413-420.
38. Zhang XM, Xue CY, Zhao FL, et al. Suitable extracellular oxidoreduction potential inhibit rex regulation and effect central carbon and energy metabolism in *Saccharopolyspora spinosa*[J]. *Microb Cell Fact*. 2014;13(1):1-11.
39. Westfall PJ, Pitera DJ, Lenihan JR, et al. Benjamin. Production of amorphadiene in yeast, and its conversion to dihydroartemisinic acid, precursor to the antimalarial agent artemisinin. *Proc Natl Acad Sci U S A*. 2012;109(3):E1111-E1118.
40. Scalcinati G, Knuf C, Partow S, et al. Dynamic control of gene expression in *Saccharomyces cerevisiae* engineered for the production of plant sesquiterpene  $\alpha$ -santalene in a fed-batch mode. *Metab Eng*. 2012; 14(2):91-103.
41. Paddon CJ, Westfall PJ, Pitera DJ, et al. High-level semi-synthetic production of the potent antimalarial artemisinin. *Nature*. 2013; 496(7446):528-532.
42. Zhang G, Cao Q, Liu J, Liu B, Li J, Li C. Refactoring  $\beta$ -amyirin synthesis in *Saccharomyces cerevisiae*. *AIChE J*. 2015;61(10):3172-3179.
43. Saimaru H, Orihara Y, Tansakul P, Kang YH, Shibuya M, Ebizuka Y. Production of triterpene acids by cell suspension cultures of *Olea europaea*. *Chem Pharm Bull*. 2007;55(5):784-788.
44. Morita M, Shibuya M, Kushiro T, Masuda K, Ebizuka Y. Molecular cloning and functional expression of triterpene synthases from pea (*Pisum sativum*). *FEBS J*. 2000;267(12):3453-3460.
45. Kirby J, Romanini DW, Paradise EM, Keasling JD. Engineering triterpene production in *Saccharomyces cerevisiae*- $\beta$ -amyirin synthase from *Artemisia annua*. *FEBS J*. 2008;275(8):1852-1859.
46. Leber R, Zenz R, Schröttner K, Fuchsbichler S, Pühlinger B, Turnowsky F. A novel sequence element is involved in the transcriptional regulation of expression of the ERG1 (squalene epoxidase) gene in *Saccharomyces cerevisiae*. *FEBS J*. 2001;268(4):914-924.
47. Favre B, Ryder NS. Cloning and expression of squalene epoxidase from the pathogenic yeast *Candida albicans*. *Gene*. 1997;189(1): 119-126.
48. Gu WL, An GH, Johnson EA. Ethanol increases carotenoid production in *Phaffia rhodozyma*. *J Ind Microbiol Biot*. 1997;19(2): 114-117.
49. Yamane Y, Higashida K, Nakashimada Y, Kakizono N T, Nishio N. Astaxanthin production by *Phaffia rhodozyma* enhanced in fed-batch culture with glucose and ethanol feeding. *Biotechnol Lett*. 1997; 19(11):1109-1111.

Manuscript received Mar. 22, 2018, and revision received Jun. 25, 2018.

